Hindawi
Advances in Civil Engineering
Volume 2023, Article ID 6615699, 10 pages
https://doi.org/10.1155/2023/6615699

Research Article

Numerical Simulation of Artificial Recharge Groundwater Effect on Overlying Soft Clay Compression Control

Chenghua Xu,[1] Dandan Yu,[1] Gang Liu,[1] Zujiang Luo,[2] and Zhao Li[2]

[1]*The 1st Geological Brigade of Jiangsu Geology and Mineral Exploration Bureau, Nanjing 210041, China*
[2]*School of Earth Sciences and Engineering, Hohai University, Nanjing 211100, China*

Correspondence should be addressed to Zhao Li; lizhao1990@hhu.edu.cn

Received 6 June 2023; Revised 9 November 2023; Accepted 10 November 2023; Published 30 November 2023

Academic Editor: Chu Zhaofei

Soil deformation is prone to occur in the process of the foundation pit dewatering. A large number of metro existing tunnels are located in soft soil layers. The compression of soft soil poses a threat to metro existing tunnels. Previously, plenty of research on foundation pit dewatering is focused on the hydraulic head and deformation characteristics of the aquifer. However, the law of water releasing and compression deformation of overlying soft soil has not been taken seriously. In order to study the artificial recharge groundwater effect on overlying soft clay, a three-dimensional seepage–soil deformation coupling numerical model was established. The theoretical basis of the model is Darcy's law and the principle of effective stress. A foundation pit located in Nanjing, China was selected as an example. The numerical model was used to simulate the hydraulic head and soil deformation caused by foundation pit dewatering and artificial recharge groundwater outside. The result shows that, due to the difference of hydraulic head between the aquifer and the aquitard reducing, it also has a good control effect on the deformation of the soft soil by recharging water into the aquifer. The location of recharge wells around the metro existing tunnel can control the soil deformation effectively, which could help to reduce the impact on the metro existing tunnel.

1. Introduction

Underground space development has been a hot issue in scientific research. Metros are constructed to relieve traffic jams in urban. Soil deformation around the tunnel is obvious, especially in soft deposit [1–3]. Grantz [4, 5] reported a number of rectangular immersed tunnels in several countries, all suffering from long-term settlements. Ng et al. [6] found a maximum tunnel settlement of 288 mm of Shanghai Metro Line 1 and 144 mm of Shanghai Metro Line 2. Too large deformation of the soil would threaten the safety of the tunnel, resulting in collapse or water inrush of the tunnel [7–9].

Previous studies investigated the settlement caused by tunnels construction [10–13]. Cooper et al. [14] reported an observed settlement of more than 12 mm for the Piccadilly Line tunnel 38 months after the completion of an underneath crossing tunnel in London, UK. Komiya et al. [15] reported that the tunnels suffered from excessive settlement due to soft clay consolidation induced by construction of a nearby embankment in Tokyo, Japan. The long-term settlement may be caused by factors such as nearby construction, cyclic train loading, and secondary compression of soft clay.

Scholars studied the measures of settlement control during nearby construction. Zhang et al. [16] presented a dual-fluid system of cement and sodium silicate of grouting-based treatment technology. A device was designed specially to avoid blocking the grouting holes. This grouting-based treatment provides an effective way to control the settlements of tunnels in soft deposits. Di et al. [17] presented three in situ grouting tests for long-term settlement treatment of a cut-and-cover tunnel of Nanjing Metro Line 10, and a bottom-up grouting sequence and a cement and water glass grout mixture are advised. Zhou et al. [18] proposed a grouting and lifting measure named "bottom grouting, inner support, real-time monitoring, and immediate adjusting" to uplift the deviated tunnel axis. Grouting was considered an effective measure to control the settlement of the tunnel generally, but the cost of grouting is quite expensive.

Nutbrown [19, 20] studied the effect of artificial recharge groundwater. Phien-wej et al. [21] conducted a field experiment

of artificial recharge groundwater to control settlement. The monitoring data showed that the recharged aquifer was rebounded. Teatini et al. [22] reviewed the fundamental geomechanical processes that govern land upheaval due to fluid recharge, and numerous examples were introduced to show the effect of fluid recharge. Zheng et al. [23] performed a series of single-well and multiwell pumping and recharge tests to discuss the effect of artificial recharge groundwater. They concluded that the twin-well combined recharge technique can be used to control the head loss of an aquifer. The effect of settlement control is studied by pumping–recharge tests and settlement monitoring. However, the existing tunnels are located in the soft soil underground, and the soft soil is generally overly the aquifer. Sarma and Xu [24] studied the factors that affect the recharge rate in arid alluvial. Huang et al. [25] conducted a site test and established a numerical model to study the soil behavior under artificial recharge, which demonstrated that artificial recharge is an effective method to control the land subsidence. It is necessary to study the effect of artificial recharge groundwater on the control of overlying soft soil deformation.

Previous studies showed that artificial recharge groundwater is an effective measure to control the settlement and aquifer deformation [26–28]. But the control effect of artificial recharge groundwater on the deformation of the overlying soft soil is lacking. The purpose of this work was to study the effect of artificial recharge groundwater on the deformation of the overlying soft soil. The main objectives of this paper are three aspects: (1) obtain the parameters of the soil by field pumping test and geotechnical test, (2) analyze the hydraulic connection between the aquifer and the soft soil, and (3) simulate the effect of artificial recharge groundwater on the control of the deformation of soft soil.

2. Methodology

2.1. Seepage Theory. Based on Darcy's law and the principle of continuity, the governing equation for groundwater seepage is expressed in Equation (1) as follows [29]:

$$\frac{\partial}{\partial x}\left(K_{xx}\frac{\partial h}{\partial x}\right)+\frac{\partial}{\partial y}\left(K_{yy}\frac{\partial h}{\partial y}\right)+\frac{\partial}{\partial z}\left(K_{zz}\frac{\partial h}{\partial z}\right)+W=S_s\frac{\partial h}{\partial t}\quad (x,y,z)\in\Omega, \tag{1}$$

where K_{xx}, K_{yy}, and K_{zz} are the hydraulic conductivities in different directions; h is the hydraulic head; W is the external source and sink flux; S_s is the specific storage; and t is time.

The initial condition can be expressed in Equation (2) as follows:

$$h(x,y,z,t)|_{t=0}=h_0(x,y,z). \tag{2}$$

The boundary conditions can be expressed in Equations (3)–(5) as follows [30]:

$$h(x,y,z,t)|_{\Gamma_1}=h_1(x,y,z,t), \tag{3}$$

$$K_{xx}\frac{\partial h}{\partial n_x}\cos(n,x)+K_{yy}\frac{\partial h}{\partial n_y}\cos(n,y)+K_{zz}\frac{\partial h}{\partial n_z}\cos(n,z)|_{\Gamma_2}=q(x,y,z,t), \tag{4}$$

$$h(x,y,z,t)=z(x,y,t)\;K\frac{\partial h}{\partial n}|_{\Gamma_3}=-\mu\frac{\partial h}{\partial t}\cos\theta, \tag{5}$$

where $h_1(x,y,z,t)$ is the constant hydraulic head on boundary Γ_1; $\cos(n,x)$, $\cos(n,y)$, and $\cos(n,z)$ are the directional cosines for the normal to the body surface; $q(x,y,z,t)$ is the known discharge in per unit area; μ is the specific yield; z is the elevation of the free surface; θ is the angle between the normal vector of the outer boundary and the perpendicular direction; Γ_1 is Dirichlet boundary condition; Γ_2 is the Neumann boundary condition; and Γ_3 is the free surface boundary condition.

2.2. Soil Consolidation Theory. The coefficient of volumetric compressibility depends on the effective stress and is expressed in Equation (6) as follows [31, 32]:

$$\Delta\sigma'=-\Delta u=-\gamma_w\Delta h, \tag{6}$$

where $\Delta\sigma'$ is variation of vertical effective stress, Δu is the variation of the pore pressure, γ_w is the specific weight of water, and Δh is the variation of the hydraulic head.

According to Terzaghi's consolidation theory, the cumulative settlement caused by dewatering could be obtained by the stratified sum method. The assumptions made in the derivation of Terzaghi's consolidation equation are as follows: the soil is homogeneous and fully saturated, soil particles and pore water are incompressible, the time lag consolidation is entirely due to the low permeability of the soil, the soil is restrained against lateral deformation, and excess pore water drains out only in the vertical direction [33]. Wu et al. [34], Shen and Xu [35], and Wu et al. [36] also solved the problems of saturated soil deformation due to water release. It is demonstrated that Terzaghi's consolidation equation could accurately simulate the soil deformation in the Yangtze River Delta Plain.

$$S=U\sum_{i=1}^{n}S_i=\sum_{i=1}^{n}\frac{\Delta\sigma_i'}{E_i}b_i, \tag{7}$$

where S is the cumulative settlement, U is the solidity of the soil, S_i is the soil deformation of each layer, and E_i is the deformation modulus of each layer. For sand, E_i is the deformation modulus. But for clay, E_i could be obtained in Equation (8) as follows:

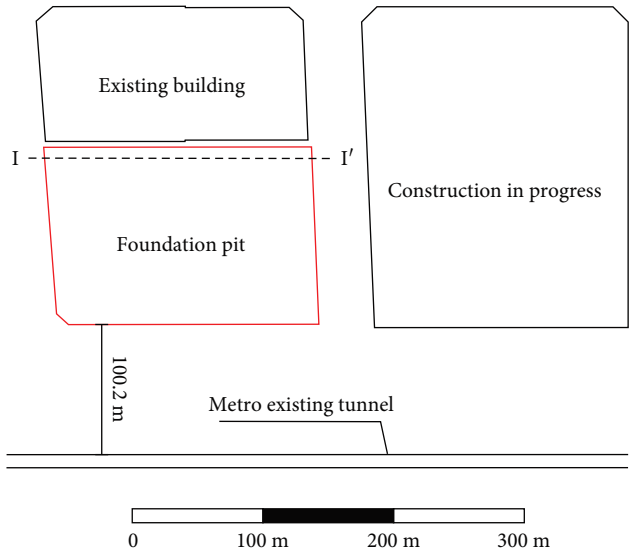

Figure 1: Site plan of the foundation pit.

$$E_i = \frac{1 + e_0}{a_v}, \tag{8}$$

where e_0 is the initial void ratio and a_v is the coefficient of volume compressibility.

3. Application

3.1. Background. The foundation pit is near the Yangtze River in Nanjing, China. The size of the foundation pit is approximately 196×128 m in plan view. The excavation depth ranges from 17.5 to 20.0 m. The tunnels of Nanjing Metro Line 1 is located 100.2 m south of the foundation pit. The site plan of the foundation pit is shown in Figure 1. The tunnel is buried at a depth from 5.4 to 11.2 m, which is situated in the clay strata. The schematic figure of the stratum and the tunnel is shown in Figure 2(a).

The soft quaternary deposits of the coastal regions of China generally consist of multi-aquifer–aquitard systems [37, 38]. The groundwater is stored in the silty fine sand, the medium coarse sand, and the gravel, which are confined aquifers. The elevation of the hydraulic head in the confined aquifer is 2.5 m. The foundation pit is close to the top of the confined aquifer. The typical cross-sectional profile, the structure of the foundation pit, and the pumping well are shown in Figure 2(b). During the excavation, the hydraulic head should be dewatered below the bottom of the foundation pit. Due to the large thickness of the confined aquifer, the diaphragm wall cannot cutoff the confined aquifer.

3.2. Conceptual Model. When the diaphragm wall is not insert into the aquifer, a depression cone with a certain shape centered on the foundation pit is to be formed during dewatering, which is similar to the formation of a depression cone of water table around the pumping well. Therefore, the distribution range of the foundation pit can be assumed to be an ideal large diameter well. The reference influence radius of the foundation pit dewatering is 615.2 m by the virtual large diameter well method [39]. In fact, the diaphragm wall of the application has been inserted into for more than two-thirds of thickness. The foundation pit dewatering would not affect beyond 615.2 m. Therefore, the scope of the simulation was extended by 700 m around the project in the process of establishing numerical model.

The model is divided into hexahedra. As the hydraulic gradient outside the foundation pit is small relatively, the mesh outside the foundation pit is set relatively large in the process of dividing the grid. Referring to previous studies [40], the mesh in the plan is set at 20 m in size outside the foundation pit, and the meshes are dense around the foundation pit, which is set at 2.5 m in size. According to the mechanical and permeability characteristics of the soil, the model is subdivided into six layers vertically that are ① impurity fill, ② silty clay, ③$_1$ silty and sand, ③$_2$ silty and sand, ④ mixed gravel medium coarse sand, and ⑤ weathered mudstone. As the model boundary is far away from the foundation pit, the surrounding boundary is treated as a constant boundary in hydraulics. The meshes, diaphragm wall, and pumping wells are shown in Figure 3. This study adopted the finite difference analysis to simulate the groundwater seepage and ground settlement.

3.3. Calibration and Validation. The field tests were taken to calibrate the parameters by comparing the measured data and the calculated data. Six pumping wells (P1–P6) and four observed wells (G4–G7) were set in the field. The structure of the pumping and observed wells is shown in Figure 2(b), and the plan location field test is shown in Figure 4. The observed well G4 was set at a different depth than the other observation wells to calibrate the hydraulic conductivity of the aquifer.

Parameter assignment has a great influence on the accuracy of the model, and fitting the calculated data with measured data is a common method to adjust parameters. Each layer was assigned initial parameters based on geotechnical test. The hydraulic parameters of the model, hydraulic conductivity, and specific storage were calibrated by a trial-and-error method to fit the calculated data with the observed data of field tests. The deformation modulus was obtained from geotechnical test. As the screens of the wells are mainly located in the ③$_1$ and ③$_2$, the parameters of the aquifers (③$_1$ and ③$_2$) were calibrated by field tests. The comparison result was shown in Figure 5. From the fitting situation, the correlation coefficient between the calculated and observed water level in the observation well under the parameter combination is 0.983. It was shown that the hydraulic head fitting situation is good. The parameters of the aquitard are based on previous scholars' studies. The parameters of the numerical model are shown in Table 1.

4. Results and Discussion

The bottom of the foundation pit is located at the bottom of the aquitard or the top of the aquifer. Therefore, the hydraulic head of the aquifer should be lowered below the bottom of the foundation pit. According to the distribution of the aquifer, diaphragm wall depth, and the situation of the existing

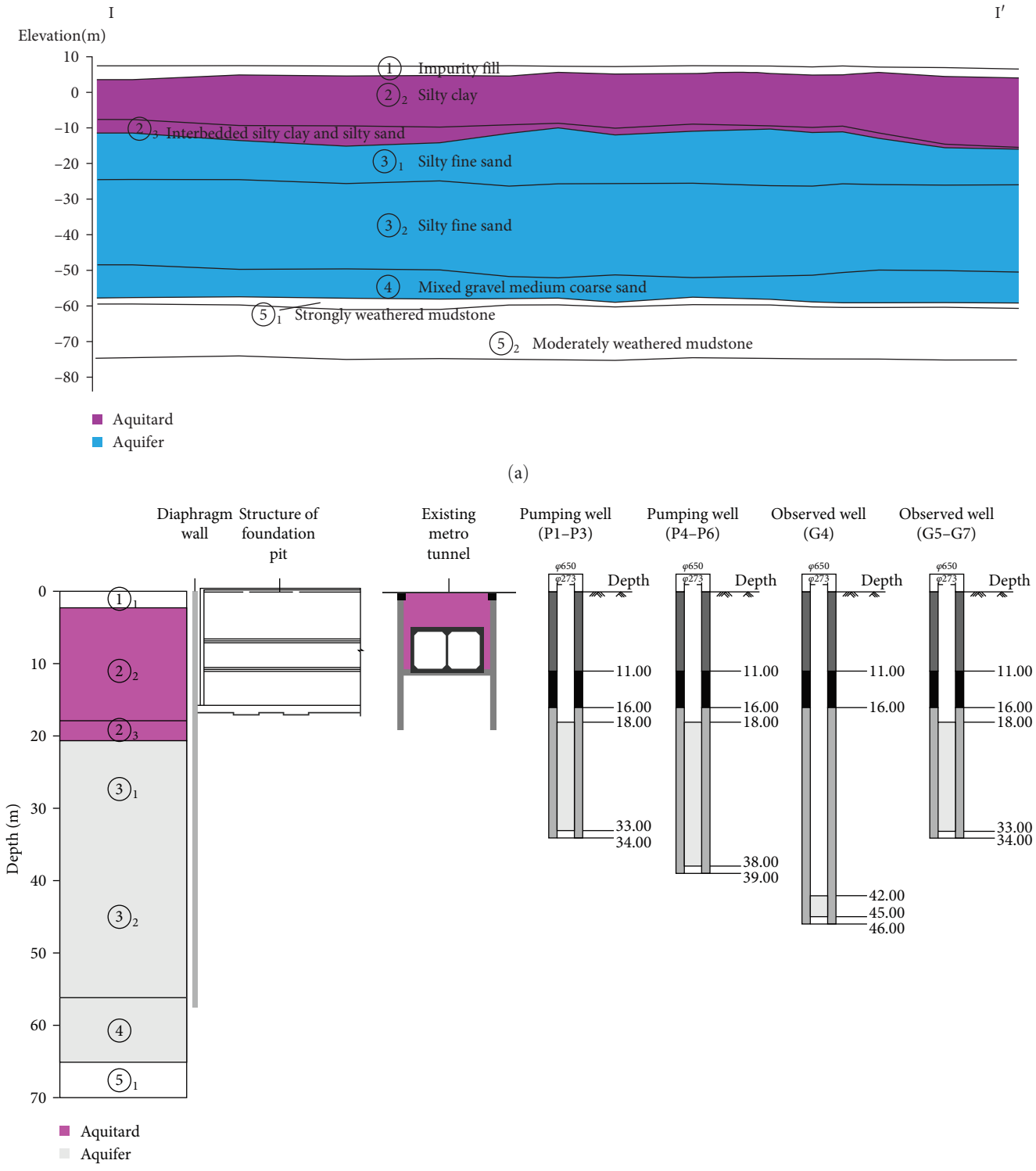

Figure 2: The typical profile of the soil, the structure of the foundation pit, the tunnel, and the pumping/recharge well. (a) The typical profile of the soil (I–I'). (b) The typical cross-sectional profile of the structure of the foundation pit, the tunnel, and the pumping/observed wells.

tunnel, the foundation pit is adopted by a suspended curtain to reduce the impact of the existing tunnel.

4.1. Foundation Pit Dewatering. The simulated results of the hydraulic head caused by dewatering are shown in Figure 6. The hydraulic head of the aquifer outside the foundation pit is −10.4 to −13.3 m. The hydraulic head of the aquifer outside the foundation pit on the south is shallower than that on the north because the diaphragm wall on the south side is deeper than that on the north side. The groundwater flow

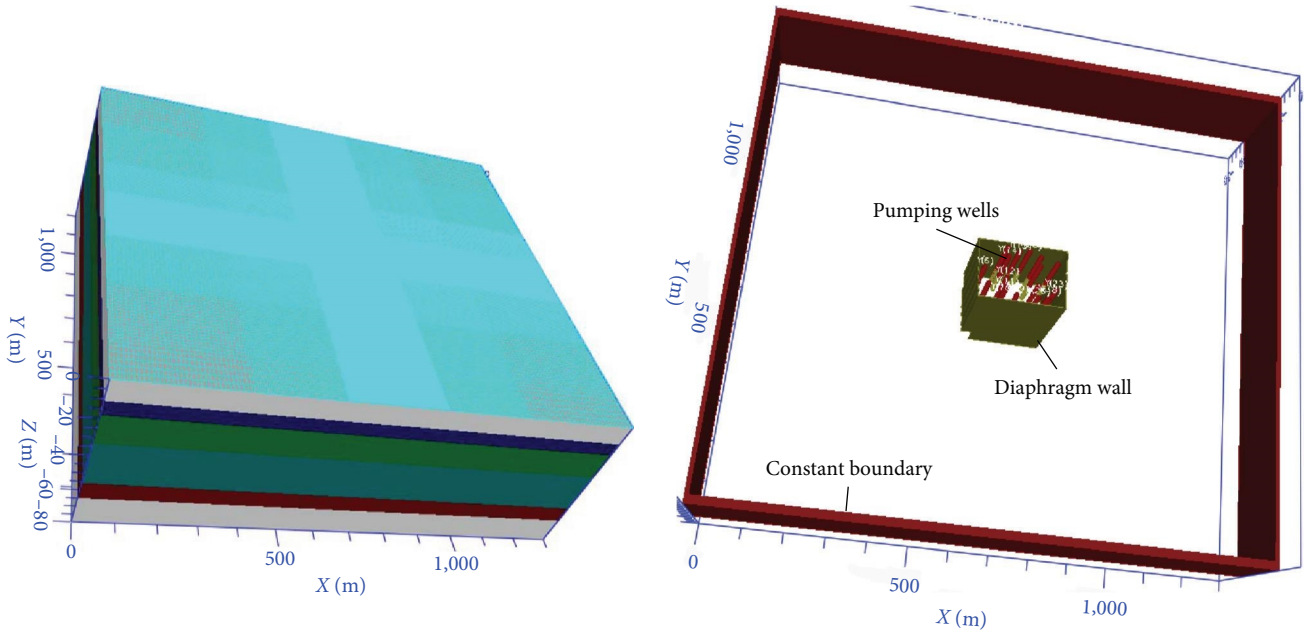

Figure 3: The numerical model. (a) The meshes of numerical model. (b) The diaphragm wall and pumping wells of numerical model.

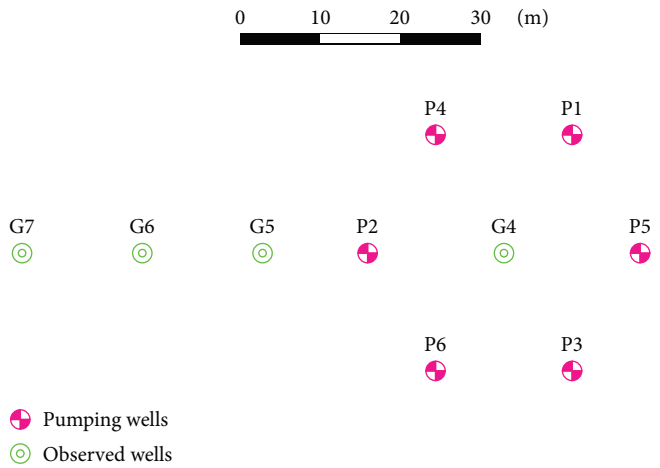

Figure 4: Plan location of field tests.

path is longer on the south than on the north side. Due to the hydraulic head difference between the aquifer and the overlying aquitard, the aquitard would compact and release water in the action of hydrodynamic force. The hydraulic head of the aquitard outside the foundation pit is −4.04 to −4.09 m.

The simulated results of the soil compression caused by dewatering are shown in Figure 7. The settlement around the foundation pit caused by dewatering is 28.5–38.2 mm. As the drawdown of the aquifer and the aquitard outside the foundation pit on the north is larger than that on the south, the settlement caused by dewatering on the north is larger. The maximum settlement at the metro existing tunnel is 25.59 mm. The compression of the aquitard caused by foundation pit dewatering is 7.22–7.50 mm. The maximum deformation of the aquitard at the metro existing tunnel is 4.04 mm.

4.2. Artificial Recharge Groundwater. Artificial recharge groundwater is a common measure to control soil deformation. In this study, two artificial recharge groundwater design schemes are studied for the effect on the settlement and the deformation of overlying aquitard, i.e., the recharge wells are arranged within the construction area (Figure 8(a)) or at the metro existing tunnel (Figure 8(b)).

The simulated results of the settlement caused by dewatering and groundwater recharge are shown in Figure 9. When the recharge wells are located near the diaphragm wall, the settlement outside the foundation pit is controlled.

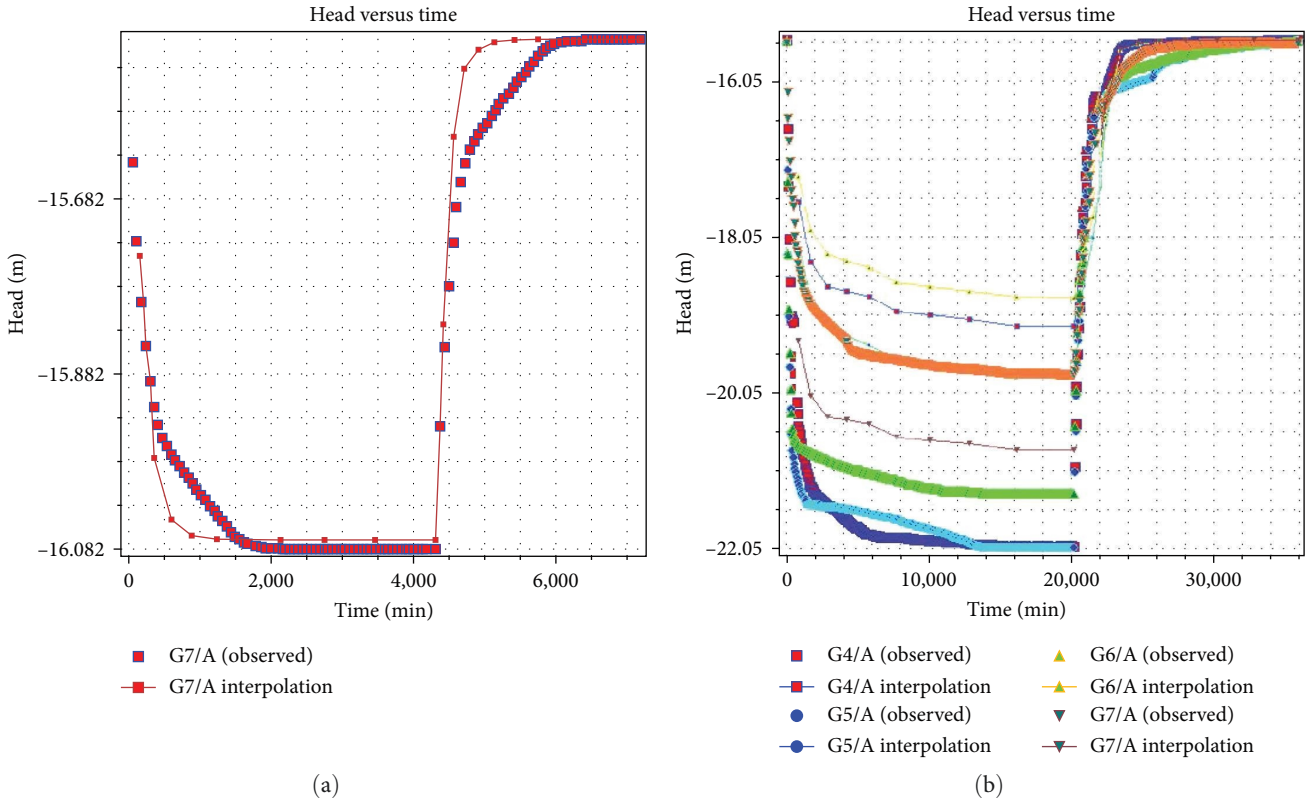

Figure 5: Scatter diagram of measured against calculated hydraulic head. (a) The comparison between measured and calculated hydraulic head during field test with one pumping well and one observed well. (b) The comparison between measured and calculated hydraulic head during field test with six pumping wells and four observed wells.

Table 1: Parameters of the numerical model.

Layer	Soil	Hydraulic conductivity (m/d)		Specific storage (1/m)	Deformation modulus (MPa)
		K_{xx} (K_{yy})	K_{zz}	S_s	E_i
1	①	0.0001	0.00001	1×10^{-6}	8
2	②	0.0002	0.00002	5×10^{-4}	8
3	$③_1$	12	3.5	5×10^{-5}	90
4	$③_2$	13	4	5×10^{-5}	95
5	④	20	5	1×10^{-4}	140
6	⑤	0.0001	0.00001	1×10^{-4}	200

As shown in Figure 9(a), the settlement at the south of the foundation pit is 7.35–16.49 mm. Compared to the settlement caused by foundation pit dewatering (without artificial recharge groundwater), the settlement near the foundation pit is reduced by 49.90%–76.03%. The settlement at the metro existing tunnel is 11.28–12.76 mm. Compared to the settlement caused by foundation pit dewatering (without artificial recharge groundwater), the settlement at the metro existing tunnel is reduced by 48.36%–55.64%.

When the recharge wells are located at the metro existing tunnel, the settlement outside the foundation pit is also controlled. As shown in Figure 9(b), the settlement at the south of the foundation pit is 19.17–21.08 mm. Compared to the settlement caused by foundation pit dewatering (without artificial recharge groundwater), the settlement near the foundation pit is reduced by 34.63%–41.81%. The settlement at the metro existing tunnel is 5.11–9.41 mm. Compared to the settlement caused by foundation pit dewatering (without artificial recharge groundwater), the settlement at the metro existing tunnel is reduced by 60.00%–79.67%.

The simulated results of the compression of the aquitard caused by dewatering and artificial recharge groundwater are shown in Figure 10. When the recharge wells are located near the diaphragm wall, the compression of the aquitard outside the foundation pit is controlled. As shown in Figure 10(a), the compression of the aquitard at the south of the foundation pit is 0.70–4.26 mm. Compared to the compression of the aquitard caused by foundation pit dewatering (without artificial

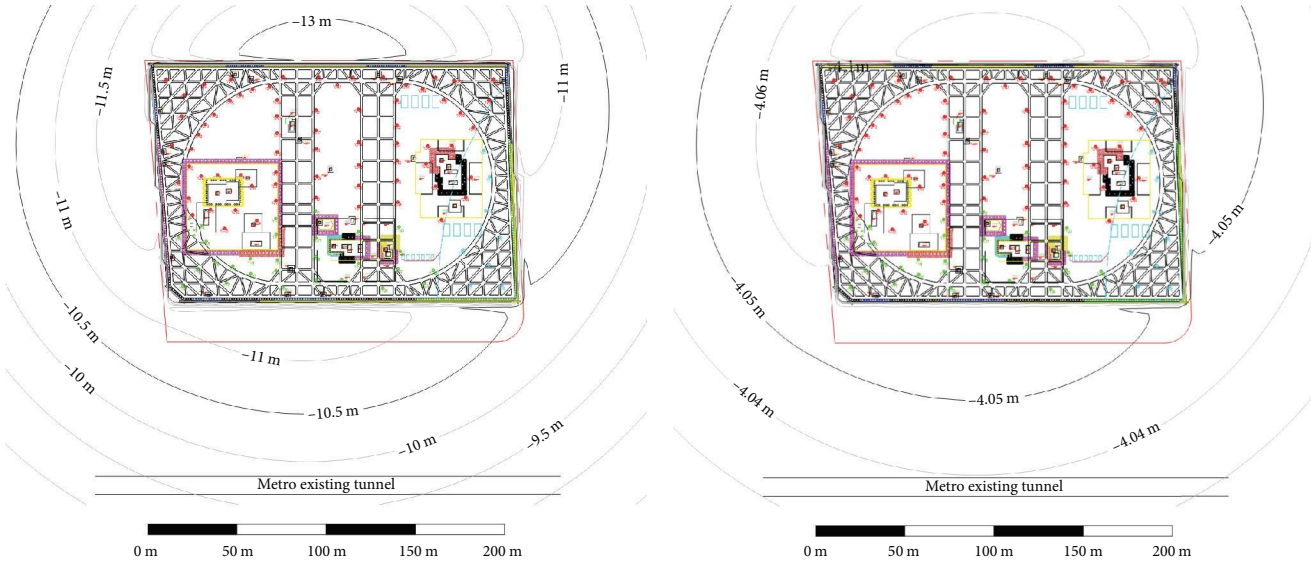

Figure 6: The simulated hydraulic head caused by foundation pit dewatering. (a) The hydraulic head of the aquifer. (b) The hydraulic head of the aquitard.

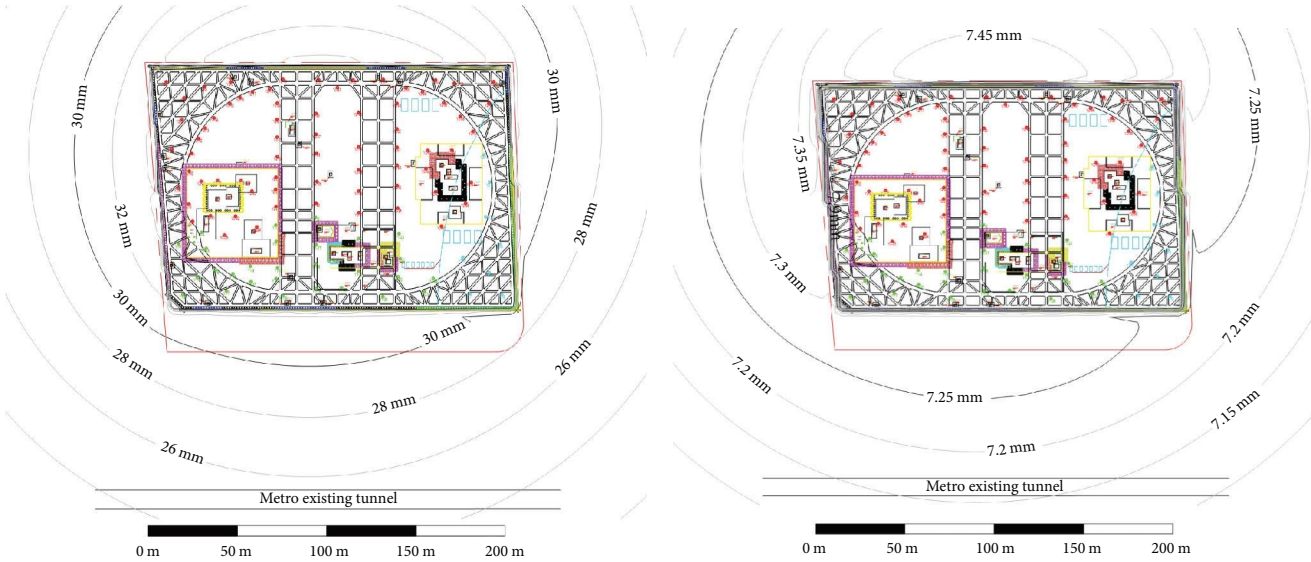

Figure 7: The simulated settlement and soil compression caused by foundation pit dewatering. (a) The settlement caused by foundation pit dewatering. (b) The compression of aquitard.

recharge groundwater), the compression of the aquitard near the foundation pit is reduced by 31.78%–90.38%. The compression of the aquitard at the metro existing tunnel is 4.5–5.2 mm. Compared to the settlement caused by foundation pit dewatering (without artificial recharge groundwater), the settlement at the metro existing tunnel is reduced by 27.73%–37.12%.

When the recharge wells are located at the metro existing tunnel, the compression of the aquitard outside the foundation pit is also controlled. As shown in Figure 10(b), the compression of the aquitard at the south of the foundation pit is 6.59–6.90 mm. Compared to the compression of the aquitard caused by foundation pit dewatering (without artificial recharge groundwater), the compression of the aquitard near the foundation pit is reduced by 4.55%–12.89%. The compression of the aquitard at the metro existing tunnel is 1.15–3.49 mm. Compared to the compression of the aquitard caused by foundation pit dewatering (without artificial recharge groundwater), the compression of the aquitard at the metro existing tunnel is reduced by 50.17%–83.79%.

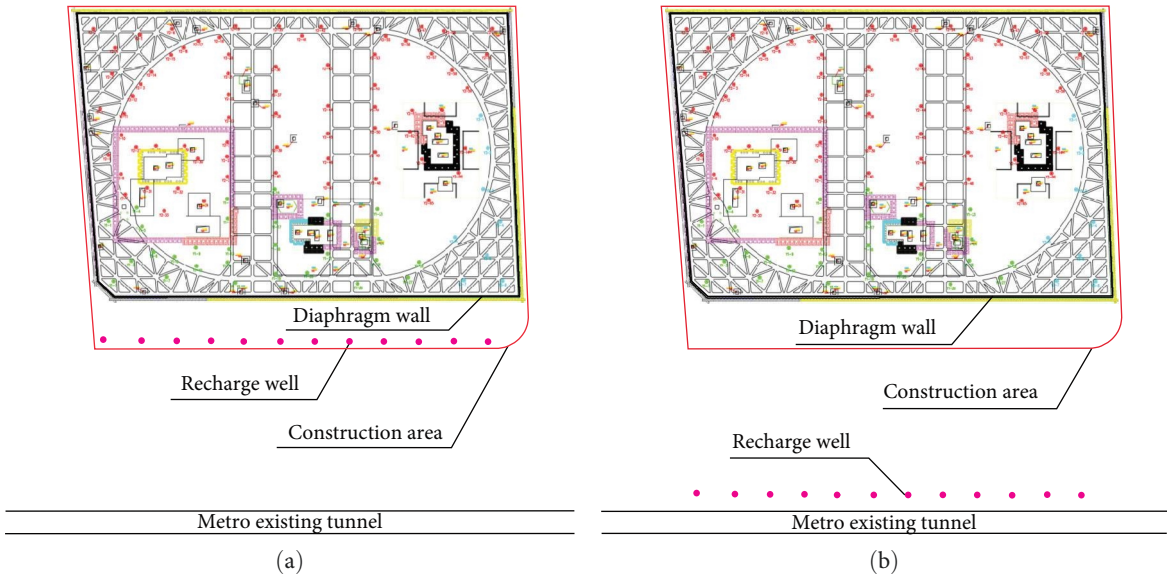

FIGURE 8: The artificial recharge groundwater scheme. (a) Recharge wells are arranged within the construction area. (b) Recharge wells are at the metro existing tunnel.

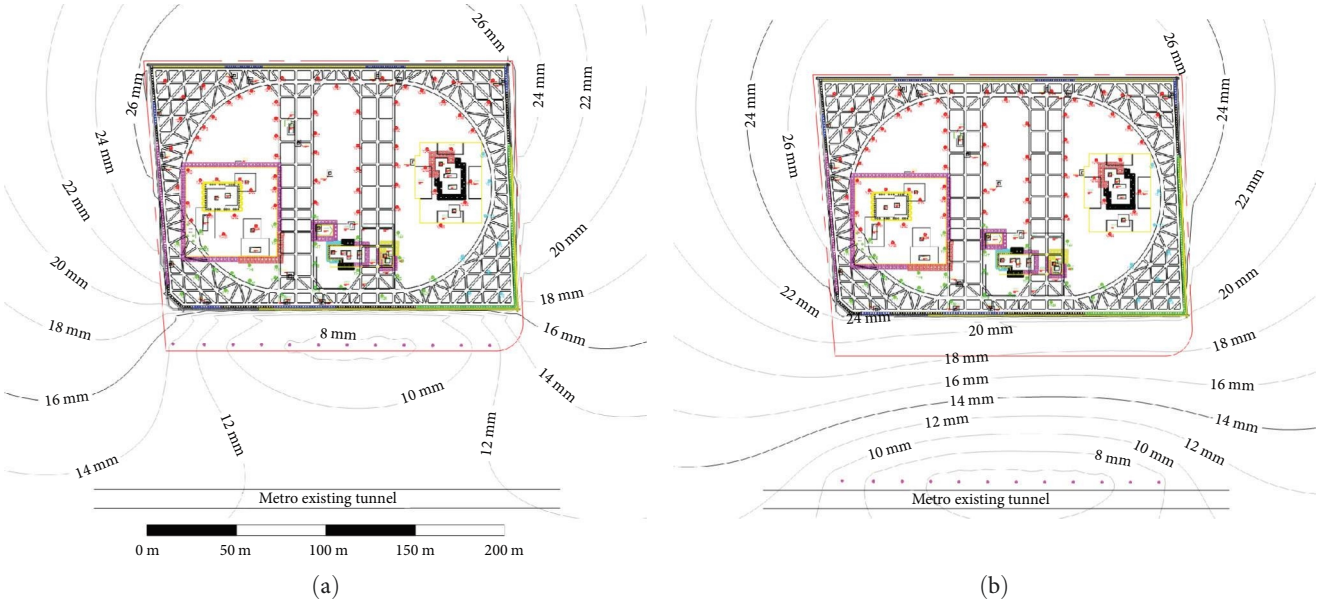

FIGURE 9: The simulated settlement caused by foundation pit dewatering and artificial recharge groundwater. (a) Recharge wells are arranged within the construction area. (b) Recharge wells are at the metro existing tunnel.

5. Conclusions

In this paper, a three-dimensional numerical model was established based on the monitoring data during pumping tests in Nanjing, China. The following conclusions are obtained from the numerical simulation:

(1) In the process of foundation pit dewatering, the hydraulic head of the aquifer decreases. Meanwhile, the hydraulic head of the overlying aquitard would also decrease due to the hydraulic head between the aquifer and the aquitard.

(2) The settlement and the compression of the aquitard outside the foundation pit could be controlled by artificial recharge groundwater. The closer the recharge wells are to the diaphragm wall, the better the control effect on settlement outside the foundation pit by comparing two artificial recharge groundwater design schemes.

(3) The layer of artificial recharge groundwater is the aquifer. Due to reducing the hydraulic head difference between the aquifer and the aquitard, it also has a good control effect on the deformation of the

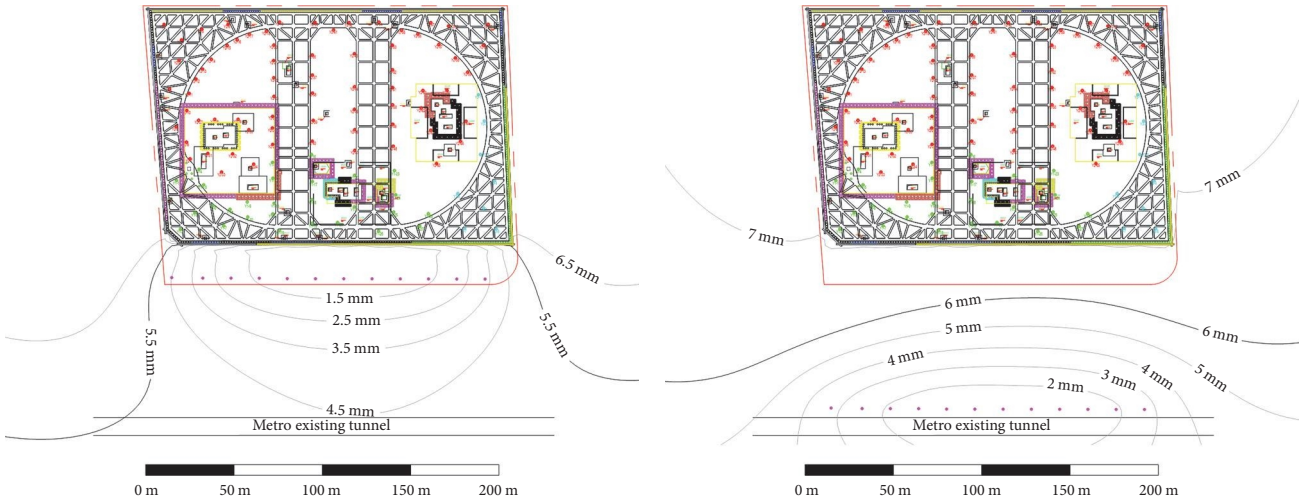

Figure 10: The simulated compression of the aquitard caused by foundation pit dewatering and artificial recharge groundwater. (a) Recharge wells are arranged within the construction area. (b) Recharge wells are at the metro existing tunnel.

aquitard. The location of recharge wells around the subway can better control the soil deformation, which could help reduce the impact on the metro existing tunnel.

Data Availability

The data supporting the conclusion of the article are shown in the relevant figures and tables in the article.

Conflicts of Interest

The authors declare that there are no conflicts of interest regarding the publication of this article.

Acknowledgments

The research work described herein was funded by Scientific and Technological Innovation Project of Jiangsu Geological Bureau, China (grant no. 2022KY01) and Jiangsu Geological Engineering Environment Intelligent Monitoring Engineering Research Center of China (grant no. 2021-ZNJKJJ-01). The corresponding author acknowledged the support of the Natural Science Foundation of Jiangsu Province, China (grant no. BK20220994), China Postdoctoral Science Foundation (grant no. 2023M730915), and Jiangsu Funding Program for Excellent Postdoctoral Talent (grant no. 2022ZB144).

References

[1] S.-L. Shen, H.-N. Wu, Y.-J. Cui, and Z.-Y. Yin, "Long-term settlement behaviour of metro tunnels in the soft deposits of Shanghai," *Tunnelling and Underground Space Technology*, vol. 40, pp. 309–323, 2014.

[2] Y.-S. Xu, L. Ma, S.-L. Shen, and W.-J. Sun, "Evaluation of land subsidence by considering underground structures that penetrate the aquifers of Shanghai, China," *Hydrogeology Journal*, vol. 20, no. 8, pp. 1623–1634, 2012.

[3] H.-W. Huang, Y.-J. Zhang, D.-M. Zhang, and B. M. Ayyub, "Field data-based probabilistic assessment on degradation of deformational performance for shield tunnel in soft clay," *Tunnelling and Underground Space Technology*, vol. 67, pp. 107–119, 2017.

[4] W. C. Grantz, "Immersed tunnel settlements. Part 1: nature of settlements," *Tunnelling and Underground Space Technology*, vol. 16, no. 3, pp. 195–201, 2001.

[5] W. C. Grantz, "Immersed tunnel settlements: Part 2: case histories," *Tunnelling and Underground Space Technology*, vol. 16, no. 3, pp. 203–210, 2001.

[6] C. W. W. Ng, G. B. Liu, and Q. Li, "Investigation of the long-term tunnel settlement mechanisms of the first metro line in Shanghai," *Canadian Geotechnical Journal*, vol. 50, no. 6, pp. 674–684, 2013.

[7] C.-J. Gong, C.-R. Xie, Z.-Q. Lin, D.-W. Xie, and Z. Zhou, "Ground deformation prediction induced by shield tunnelling considering existing multi-story buildings," *Journal of Central South University*, vol. 30, no. 4, pp. 1373–1387, 2023.

[8] Z. Li, Z. Luo, C. Xu, and J. Tan, "3D fluid-solid full coupling numerical simulation of soil deformation induced by shield tunnelling," *Tunnelling and Underground Space Technology*, vol. 90, pp. 174–182, 2019.

[9] C. Yong, D. Jinlong, G. Fei et al., "Review of landslide susceptibility assessment based on knowledge mapping," *Stochastic Environmental Research and Risk Assessment*, vol. 36, no. 9, pp. 2399–2417, 2022.

[10] R. B. Peck, "Deep excavations and tunneling in soft ground," in *7th International Conference on Soil Mechanics and Foundation Engineering (Mexico)*, pp. 225–290, SIMSG ISSMGE, Mexico, 1969.

[11] Z. Luo, Z. Li, J. Tan, Q. Ma, and Y. Hu, "Three-dimensional fluid–soil full coupling numerical simulation of ground settlement caused by shield tunnelling," *European Journal of Environmental and Civil Engineering*, vol. 24, no. 8, pp. 1261–1275, 2020.

[12] D. Bouayad and F. Emeriault, "Modeling the relationship between ground surface settlements induced by shield tunneling and the operational and geological parameters based on the hybrid PCA/ANFIS method," *Tunnelling and Underground Space Technology*, vol. 68, pp. 142–152, 2017.

[13] N.-A. Do, D. Dias, P. Oreste, and I. Djeran-Maigre, "Three-dimensional numerical simulation of a mechanized twin tunnels in soft ground," *Tunnelling and Underground Space Technology*, vol. 42, pp. 40–51, 2014.

[14] M. L. Cooper, D. N. Chapman, C. D. F. Rogers, and A. H. C. Chan, "Movements in the piccadilly line tunnels due to the heathrow express construction," *Géotechnique*, vol. 52, no. 4, pp. 243–257, 2002.

[15] K. Komiya, K. Takiyama, and H. Akagi, "Settlement behaviour of a shield tunnel constructed in subsiding reclaimed area," in *Geotechnical Aspects of Underground Construction in Soft Ground - Proceedings of the 5th International Conference of TC28 of the ISSMGE*, pp. 239–244, ISSMGE, Amsterdam, The Netherlands, June 2005.

[16] D.-M. Zhang, Z.-K. Huang, R.-L. Wang, J.-Y. Yan, and J. Zhang, "Grouting-based treatment of tunnel settlement: practice in Shanghai," *Tunnelling and Underground Space Technology*, vol. 80, pp. 181–196, 2018.

[17] H. Di, S. Zhou, X. Yao, and Z. Tian, "In situ grouting tests for differential settlement treatment of a cut-and-cover metro tunnel in soft soils," *Bulletin of Engineering Geology and the Environment*, vol. 80, no. 8, pp. 6415–6427, 2021.

[18] S. Zhou, J. Xiao, H. Di, and Y. Zhu, "Differential settlement remediation for new shield metro tunnel in soft soils using corrective grouting method: case study," *Canadian Geotechnical Journal*, vol. 55, no. 12, pp. 1877–1887, 2018.

[19] D. A. Nutbrown, "Normal mode analysis of the linear equation of groundwater flow," *Water Resources Research*, vol. 11, no. 6, pp. 979–987, 1975.

[20] D. A. Nutbrown, "A model study of the effects of artificial recharge," *Journal of Hydrology*, vol. 31, no. 1-2, pp. 57–65, 1976.

[21] N. Phien-wej, P. H. Giao, and P. Nutalaya, "Field experiment of artificial recharge through a well with reference to land subsidence control," *Engineering Geology*, vol. 50, no. 1-2, pp. 187–201, 1998.

[22] P. Teatini, G. Gambolati, M. Ferronato, A. T. Settari, and D. Walters, "Land uplift due to subsurface fluid injection," *Journal of Geodynamics*, vol. 51, no. 1, pp. 1–16, 2011.

[23] G. Zheng, J. R. Cao, X. S. Cheng, D. Ha, and F. J. Wang, "Experimental study on the artificial recharge of semiconfined aquifers involved in deep excavation engineering," *Journal of Hydrology*, vol. 557, pp. 868–877, 2018.

[24] D. Sarma and Y. Xu, "The recharge process in alluvial strip aquifers in arid Namibia and implication for artificial recharge," *Hydrogeology Journal*, vol. 25, no. 1, pp. 123–134, 2017.

[25] Y. Huang, Y. Yang, and J. Li, "Numerical simulation of artificial groundwater recharge for controlling land subsidence," *KSCE Journal of Civil Engineering*, vol. 19, no. 2, pp. 418–426, 2015.

[26] J. Wang, Y. Wu, X. Zhang, Y. Liu, T. Yang, and B. Feng, "Field experiments and numerical simulations of confined aquifer response to multi-cycle recharge-recovery process through a well," *Journal of Hydrology*, vol. 464–465, pp. 328–343, 2012.

[27] I. S. Zektser, E. Y. Potapova, A. V. Chetverikova, and R. S. Shtengelov, "Perspectives of artificial recharge of groundwater in southern European Russia," *Water Resources*, vol. 39, no. 6, pp. 672–684, 2012.

[28] Y.-Q. Zhang, J.-H. Wang, J.-J. Chen, and M.-G. Li, "Numerical study on the responses of groundwater and strata to pumping and recharge in a deep confined aquifer," *Journal of Hydrology*, vol. 548, pp. 342–352, 2017.

[29] Y.-X. Wu, S.-L. Shen, and D.-J. Yuan, "Characteristics of dewatering induced drawdown curve under blocking effect of retaining wall in aquifer," *Journal of Hydrology*, vol. 539, pp. 554–566, 2016.

[30] Z. Li, Z. Luo, Q. Wang, J. Du, W. Lu, and D. Ning, "A three-dimensional fluid-solid model, coupling high-rise building load and groundwater abstraction, for prediction of regional land subsidence," *Hydrogeology Journal*, vol. 27, no. 4, pp. 1515–1526, 2019.

[31] Y.-X. Wu, S.-L. Shen, H.-N. Wu, Y.-S. Xu, Z.-Y. Yin, and W.-J. Sun, "Environmental protection using dewatering technology in a deep confined aquifer beneath a shallow aquifer," *Engineering Geology*, vol. 196, pp. 59–70, 2015.

[32] C. Gong, Y. Wang, Y. Peng et al., "Three-dimensional coupled hydromechanical analysis of localized joint leakage in segmental tunnel linings," *Tunnelling and Underground Space Technology*, vol. 130, Article ID 104726, 2022.

[33] K. Terzaghi, *Theoretical Soil Mechanics*, John Wiley & Sons, Inc., New York, 1943.

[34] J. Wu, X. Shi, S. Ye et al., "Numerical simulation of viscoelastoplastic land subsidence due to groundwater overdrafting in Shanghai, China," *Journal of Hydrologic Engineering*, vol. 15, no. 3, pp. 223–236, 2010.

[35] S.-L. Shen and Y.-S. Xu, "Numerical evaluation of land subsidence induced by groundwater pumping in Shanghai," *Canadian Geotechnical Journal*, vol. 48, no. 9, pp. 1378–1392, 2011.

[36] H.-N. Wu, S.-L. Shen, and J. Yang, "Identification of tunnel settlement caused by land subsidence in soft deposit of Shanghai," *Journal of Performance of Constructed Facilities*, vol. 31, no. 6, 2017.

[37] Z. Li, Z. Luo, Y. Wang, G. Fan, and J. Zhang, "Suitability evaluation system for the shallow geothermal energy implementation in region by Entropy Weight Method and TOPSIS method," *Renewable Energy*, vol. 184, pp. 564–576, 2022.

[38] C. Zhuang, Z. Zhou, W. A. Illman, and J. Wang, "Geostatistical inverse modeling for the characterization of aquitard heterogeneity using long-term multi-extensometer data," *Journal of Hydrology*, vol. 578, Article ID 124024, 2019.

[39] Z. Xu, T. Chen, J. Li et al., "Defects and improvement of predicting mine water inflow by virtual large diameter well method," *Geofluids*, vol. 2022, Article ID 3067983, 11 pages, 2022.

[40] Z. Li, Z. Luo, L. Cheng, Y. Wang, G. Fan, and H. Guo, "Influence of Groundwater Heat Pump system operation on geological environment by Hydro-Thermal–Mechanical–Chemical numerical model," *Applied Thermal Engineering*, vol. 206, Article ID 118035, 2022.